Electronic Supplementary Material (ESI) for Metallomics.

Supporting Information

Positive and negative nano-electrospray mass spectrometry of ruthenated serum albumin supported by docking studies: an integrated approach towards defining metallodrug binding sites on proteins

Marija Nišavić[a], Goran Janjić[b], Amela Hozić[c], Marijana Petković[a], Zoran Vujčić[d], Miloš Milčić[d], and Mario Cindrić[c]*

[a]Department of Physical Chemistry, "Vinča" Institute of Nuclear Sciences, University of Belgrade, Mike Petrovića Alasa 12-14, 11000 Belgrade, Serbia

[b]Institute of Chemistry, Technology and Metallurgy, University of Belgrade, Njegoseva 12, 11000 Belgrade, Serbia

[c]Centre for Proteomics and Mass Spectrometry, Division of Molecular Medicine, Ruđer Bošković Institute, Bijenička cesta 54, 10000 Zagreb, Croatia

[d]Faculty of Chemistry, University of Belgrade, Studentski trg 12-14, 11000 Belgrade, Serbia

**Correspondence to: mario.cindric@irb.hr*

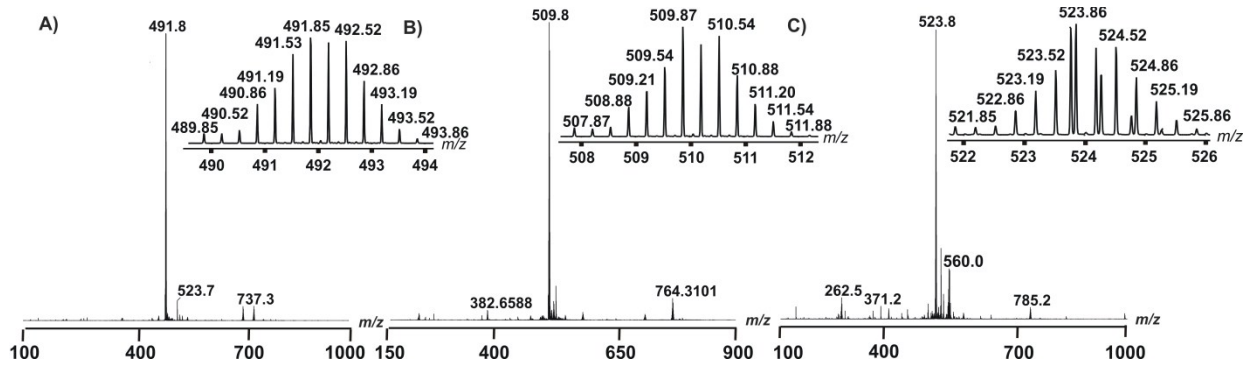

Fig. S1. Positive ion mode ESI MS spectra of angiotensin II adducts with compounds [Ru(Cl-tpy)(en)Cl]$^+$ (A), [Ru(Cl-tpy)(dach)Cl]$^+$ (B) and [Ru(Cl-tpy)(bipy)Cl]$^+$ (C). Inset in each spectrum shows isotopic distribution of triply charged ruthenated peptide. Additional peaks at *m/z* 737.3, 764.3 and 785.2 for compounds en, dach and bipy, respectively, correspond to doubly charged ruthenated angiotensin II.

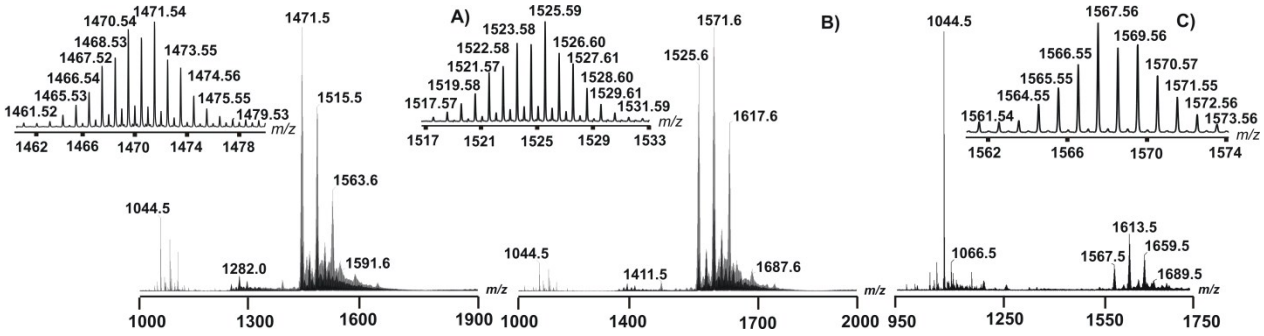

Fig. S2. Negative ion mode ESI MS spectra of angiotensin II adducts with compounds [Ru(Cl-tpy)(en)Cl]$^+$ (A), [Ru(Cl-tpy)(dach)Cl]$^+$ (B) and [Ru(Cl-tpy)(bipy)Cl]$^+$ (C). Inset in each spectrum shows isotopic distribution of singly charged ruthenated peptide. Two subsequent peaks in each spectrum (at *m/z* 1515.5 and 1563.6 for en compound, 1571.6 and 1617.6 for dach and 1613.5 and 1659.5 for bipy compound) represent mono- and di-formic acid adducts. Signal at 1044.5 in each spectrum correspond to free angiotensin II.

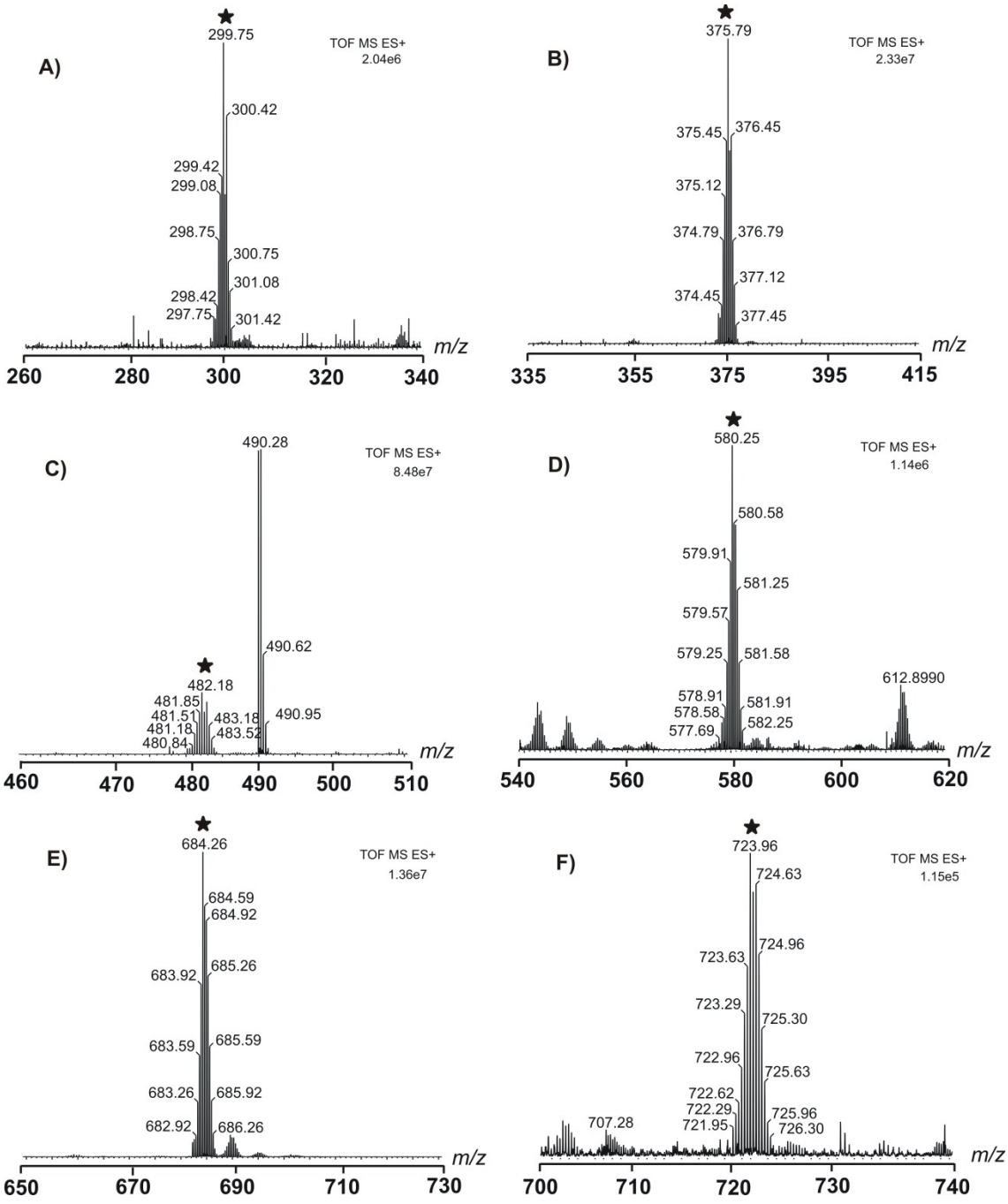

Fig. S3. Enlarged positive ion mode LE MS^E spectra showing [Ru(Cl-tpy)(en)]-bound HSA sequences: DAHK (A), SEVAHR (B), SLHTLFGDK (C), HPDYSVVLLLR (D), DVFLGMFLYEYAR (E) and HPYFYAPELLFFAK (F). Target sequences are marked with a black asterisk in each spectrum.

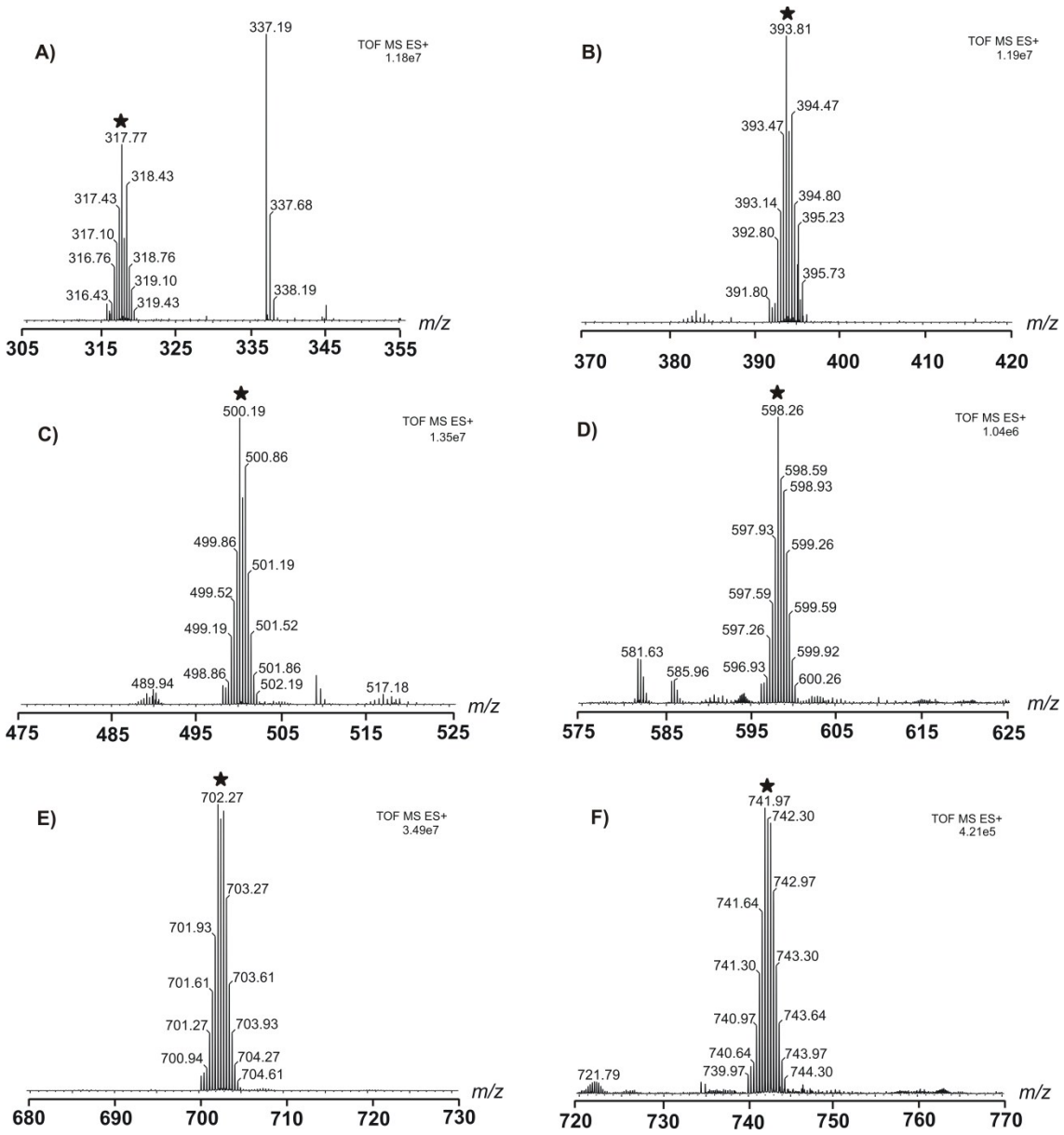

Fig. S4. Enlarged positive ion mode LE MS^E spectra showing [Ru(Cl-tpy)(dach)]-bound HSA sequences: DAHK (A), SEVAHR (B), SLHTLFGDK (C), HPDYSVVLLLR (D), DVFLGMFLYEYAR (E) and HPYFYAPELLFFAK (F). Target sequences are marked with a black asterisk in each spectrum.

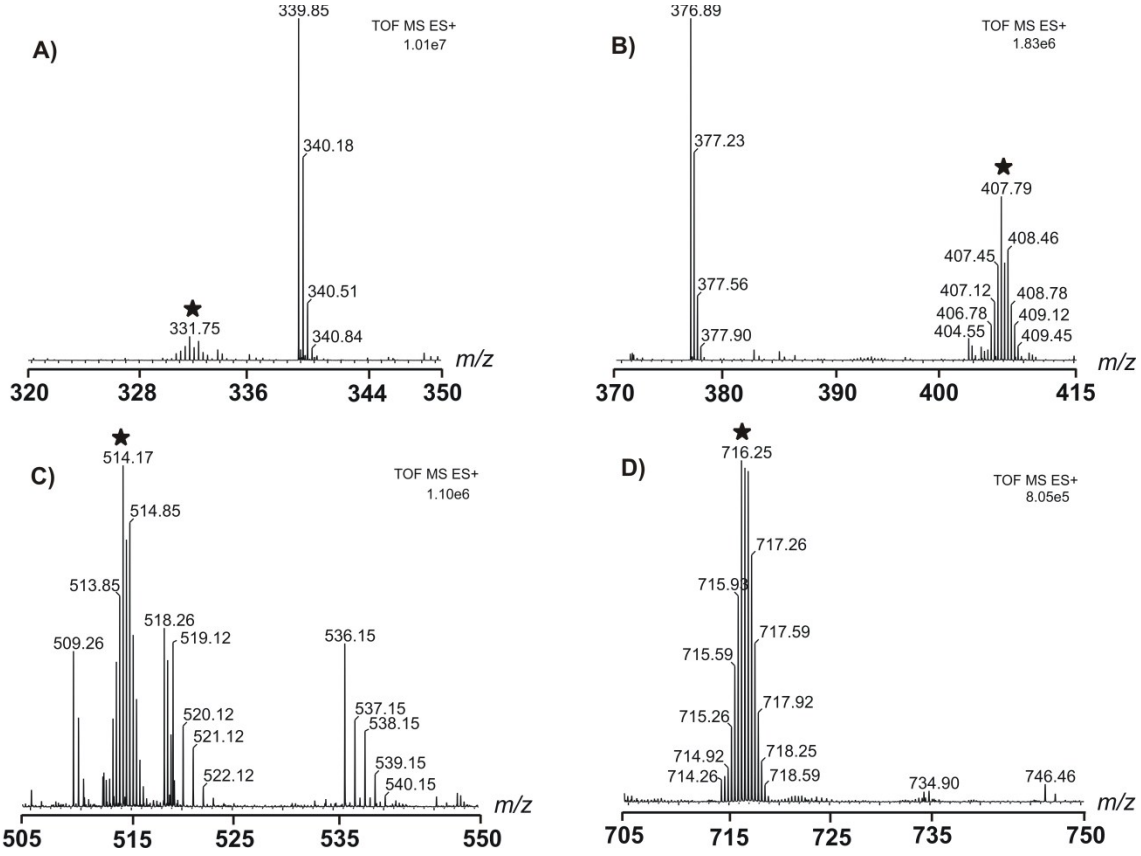

Fig. S5. Enlarged positive ion mode LE MS^E spectra showing [Ru(Cl-tpy)(bipy)]-bound HSA sequences: DAHK (A), SEVAHR (B), SLHTLFGDK (C) and DVFLGMFLYEYAR (D). Target sequences are marked with a black asterisk in each spectrum.

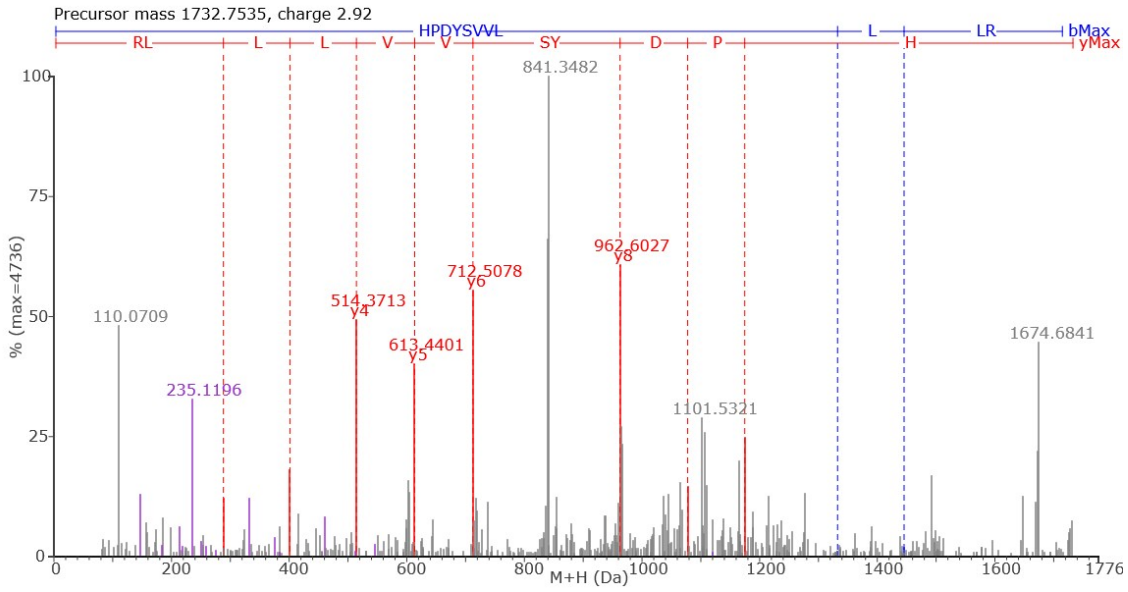

Fig. S6. PLGS generated HE MS^E spectrum of ^{338}HPDYSVVLLLR^{348} HSA sequence adduct with compound [Ru(Cl-tpy)(en)Cl]$^+$. The identified precursor is triply positively charged ion with a mass of 1732 Da. The identified mass corresponds to the peptide adduct with compound [Ru(Cl-tpy)(en)Cl]$^+$, after Cl ligand hydrolysis.

Table S1. PLGS software identified HE MS^E peptide fragment ions. marks neutral loss (H_2O, NH_3).

Peptide sequence	Number of ions	Fragment ion identity
^{5}SEVAHR^{10}	12	b_2, b_3, b_3, b_4, b_4, b_5,y_2, y_3, y_4, y_5, y_5, y_6
^{65}SLHTLFGDK^{73}	9	y_2, y_2, y_3, y_3, y_4, y_5, y_6, y_7, y_7
^{146}HPYFYAPELLFFAK^{159}	10	b_{10}, y_2, y_3, y_4, y_6, y_7, y_8, y_{12}, y_{13}, y_{14}
^{324}DVFLGMFLYEYAR^{336}	7	b_1, b_{11}, y_8, y_9, y_{10}, y_{11}, y_{12}
^{338}HPDYSVVLLLR^{348}	13	b_2, b_5, y_2, y_3, y_4, y_5, y_6, y_7, y_8, y_8, y_9, y_{10}, y_{11}

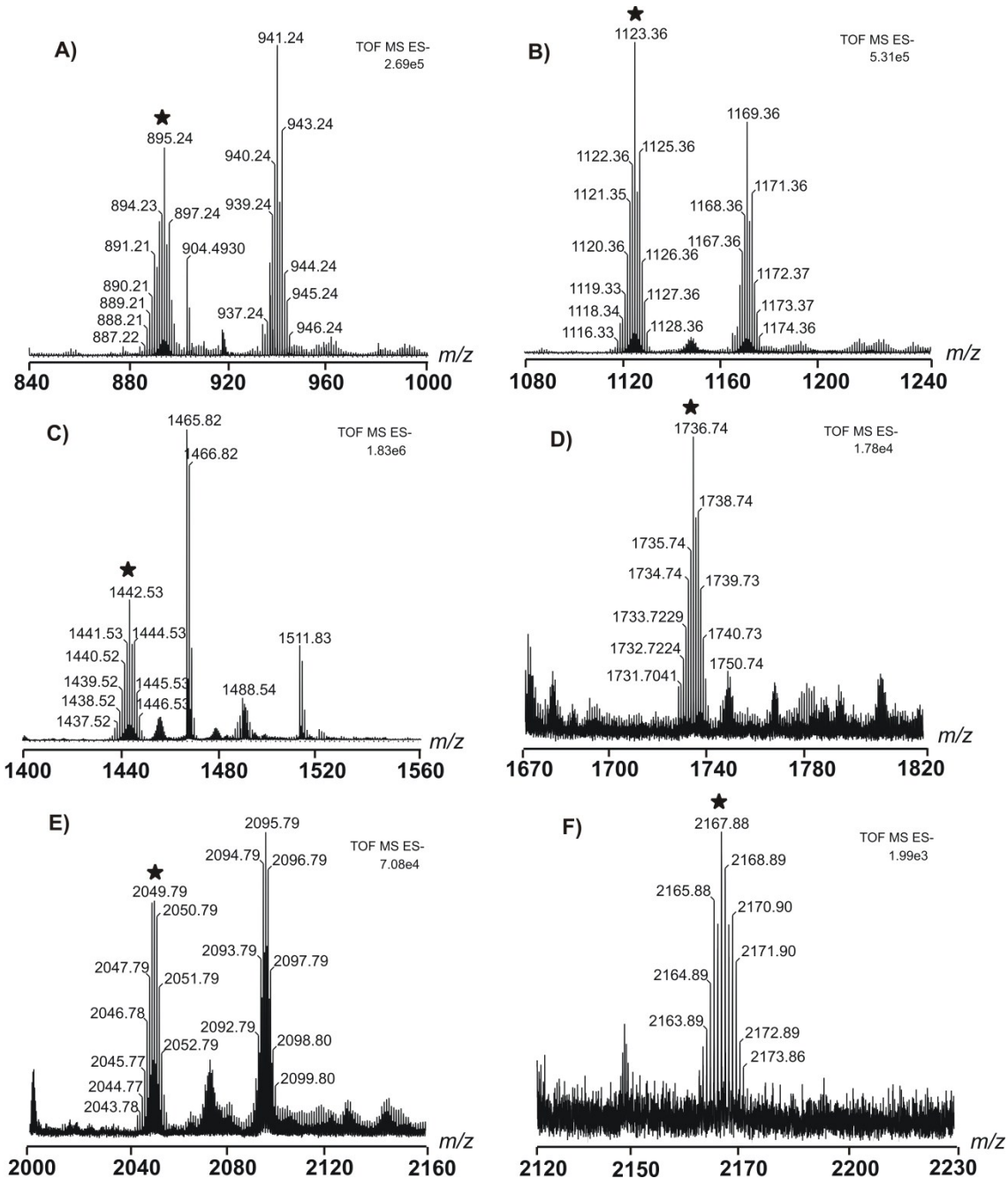

Fig. S7. Enlarged negative ion mode LE MS^E spectra showing [Ru(Cl-tpy)(en)]-bound HSA sequences: DAHK (A), SEVAHR (B), SLHTLFGDK (C), HPDYSVVLLLR (D), DVFLGMFLYEYAR (E) and HPYFYAPELLFFAK (F). Target sequences are marked with a black asterisk in each spectrum.

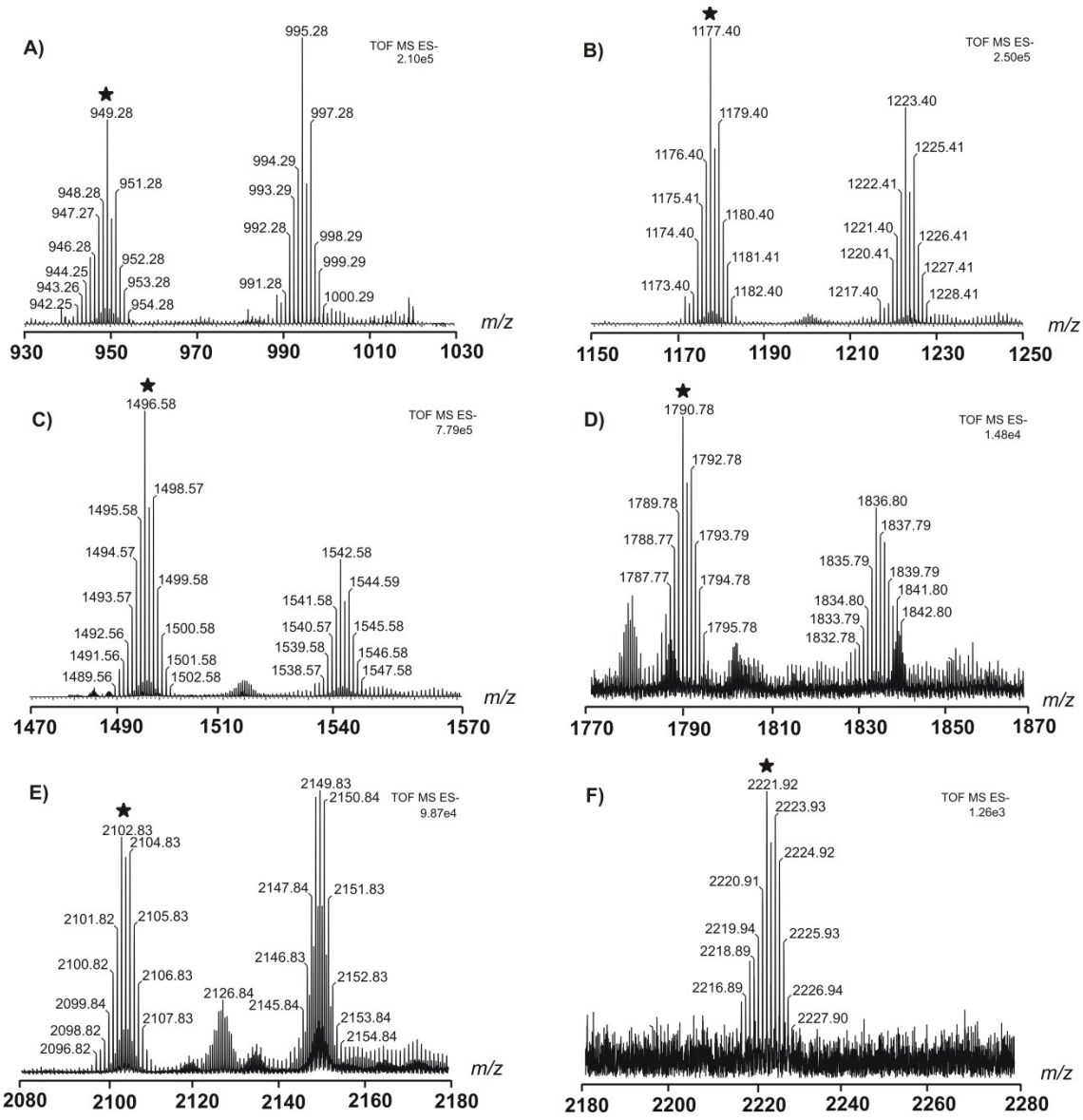

Fig. S8. Enlarged negative ion mode LE MS^E spectra showing [Ru(Cl-tpy)(dach)]-bound HSA sequences: DAHK (A), SEVAHR (B), SLHTLFGDK (C), HPDYSVVLLLR (D), DVFLGMFLYEYAR (E) and HPYFYAPELLFFAK (F). Target sequences are marked with a black asterisk in each spectrum.

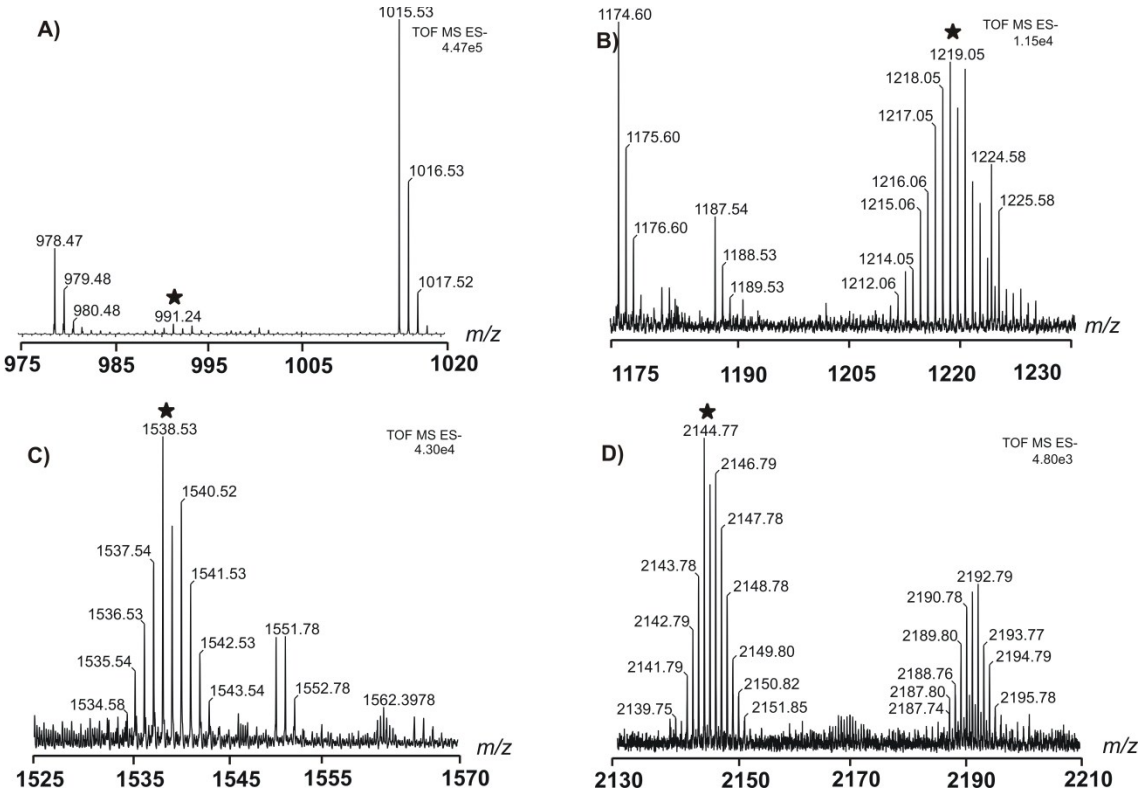

Fig. S9. Enlarged negative ion mode LE MS^E spectra showing [Ru(Cl-tpy)(dach)]-bound HSA sequences: DAHK (A), SEVAHR (B), SLHTLFGDK (C) and DVFLGMFLYEYAR (D). Target sequences are marked with a black asterisk in each spectrum.

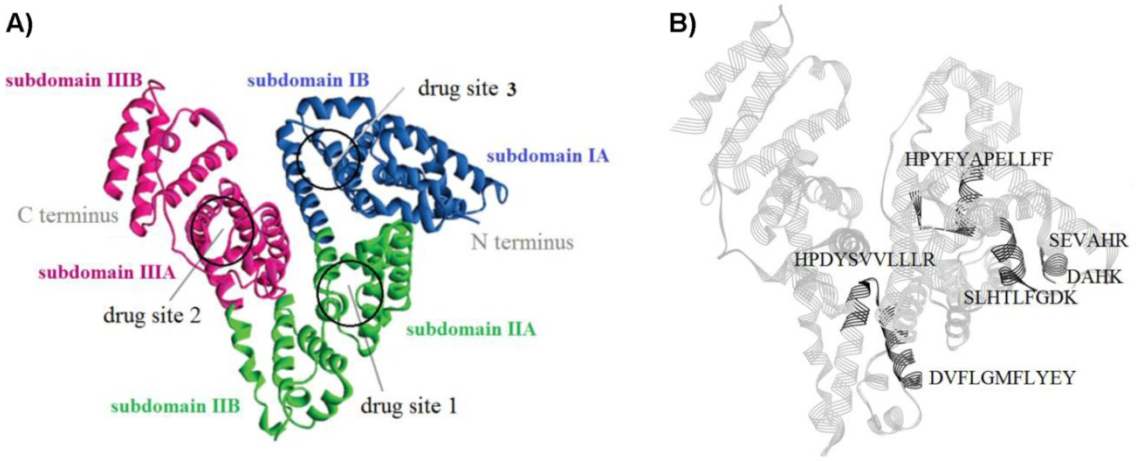

Fig. S10. HSA structure with major drug binding sites (A) and spatial localisation of MS-identified sequences for the binding of compounds $[Ru(Cl\text{-}tpy)(en)Cl]^+$, $[Ru(Cl\text{-}tpy)(dach)Cl]^+$ and $[Ru(Cl\text{-}tpy)(bipy)Cl]^+$.

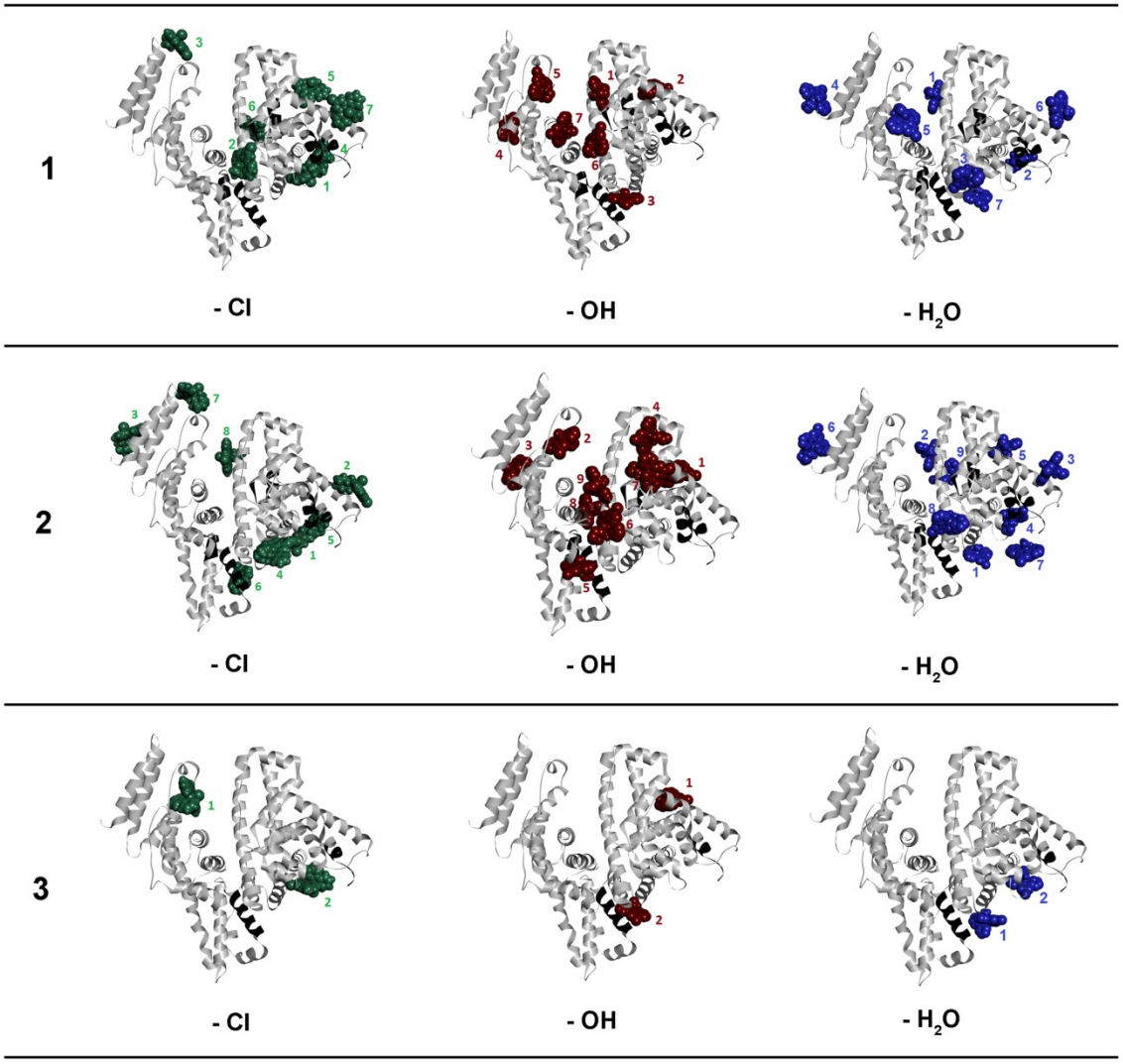

Fig. S11. HSA binding sites for chloro, hydroxo and aqua forms of compounds $[Ru(Cl\text{-}tpy)(en)Cl]^+$, $[Ru(Cl\text{-}tpy)(dach)Cl]^+$ and $[Ru(Cl\text{-}tpy)(bipy)Cl]^+$. Chloro forms are shown green, hydroxo red and aqua forms are shown blue. Target MS-identified HSA sequences are highlighted black.

Table S3. Binding energies of chloro, hydroxo and aqua forms of compounds $[Ru(Cl\text{-}tpy)(en)Cl]^+$, $[Ru(Cl\text{-}tpy)(dach)Cl]^+$ and $[Ru(Cl\text{-}tpy)(bipy)Cl]^+$, for each HSA binding site. Binding energies of chloro complexes that correspond to MS-identified sequences are highlighted green, while hydroxo complexes are marked red. The remaining binding energy values that most probably correspond to non-covalent interactions are black.

Ru(II) compound	**Binding site No**	**Binding energy (kcal/mol)**		
		-Cl	**-OH**	**-H_2O**
1 *[RuL(4'-Cl-tpy)(en)]*	1	-8,12	-7,80	-7,90
	2	-7,27	-6,32	-7,83
	3	-7,22	-5,84	-7,40
	4	-7,09	-5,77	-
	5	-6,99	-5,42	-
	6	-6,83	-5,34	-
	7	-6,74	-5,22	-
2 *[RuL(4'-Cl-tpy)(dach)]*	1	-9,14	-8,56	-3,02
	2	-8,67	-7,75	-2,95
	3	-8,53	-7,08	-2,73
	4	-8,53	-6,93	-2,66
	5	-8,38	-6,82	-
	6	-8,37	-6,77	-
	7	-7,46	-6,55	-
	8	-7,18	-6,48	-
	9	-	-6,47	-
3 *[RuL(4'-Cl-tpy)(bipy)]*	1	-7,97	-6,33	-1,78
	2	-6,98	-5,84	-1,44